State Estimation Sensitivity Analysis

Roberto Mínguez, and Antonio J. Conejo, *Fellow, IEEE*

***Abstract*— Within energy management systems, state estimation is a key function for building a network real-time model, which is a quasi-static mathematical representation of the current conditions in an interconnected network. The obtained model is dependent on the assumptions, and sensitivity analysis can be used to show how measurement schemes, transmission line modeling and other parameters affect the quality of the state estimation solution. This paper provides expressions to compute all these sensitivities, and an example and a case study are used to illustrate them.**

***Index Terms*— Energy management system, Least square estimation, Power system state estimation, Sensitivity analysis.**

NOTATION

The main notation used throughout the paper is stated below for quick reference. Other symbols are defined as required in the text.

A. State variables

v_i Voltage magnitude at bus i.
θ_i Voltage angle at bus i.

B. Dependent variables

P_i Active power injection at bus i.
Q_i Reactive power injection at bus i.
P_{ij} Active power flow from bus i to bus j.
Q_{ij} Reactive power flow from bus i to bus j.

C. Vectors

$\boldsymbol{y}$ Vector of state variables.
$\boldsymbol{x}$ Vector of variables.
$\boldsymbol{a}$ Data vector.

D. Functions

$J(\cdot)$ Quadratic measurement error function.

E. Measurements

v_i^m Voltage magnitude measurement at bus i.
P_i^m Active power injection measurement at bus i.
Q_i^m Reactive power injection measurement at bus i.
P_{ij}^m Active power flow measurement from bus i to j.
Q_{ij}^m Reactive power flow measurement from bus i to j.

Authors are partly supported by the Ministry of Science and Education of Spain through CICYT projects DPI2003-01362 and BIA2005-07802-C02-01, and by the Junta de Comunidades de Castilla-La Mancha, through project PBI-05-053.

R. Mínguez and A. J. Conejo are with the University of Castilla-La Mancha, Ciudad Real, Spain. (e-mails: Roberto.Minguez@uclm.es, Antonio.Conejo@uclm.es).

F. Weighting factors

w_i^V Weighting factor for voltage measurement at bus i.
w_i^P Weighting factor for active power injection measurement at bus i.
w_i^Q Weighting factor for reactive power injection measurement at bus i.
w_{ij}^P Weighting factor for active power flow measurement from bus i to j.
w_{ij}^Q Weighting factor for reactive power flow measurement from bus i to j.

G. Physical limits

$P_i^{\max}$ Maximum active power generation at bus i.
$Q_i^{\max}$ Maximum reactive power generation at bus i.
$P_i^{\min}$ Minimum active power generation at bus i.
$Q_i^{\min}$ Minimum reactive power generation at bus i.

H. Constants

$\boldsymbol{x}^e$ Vector of variable estimates.
$\boldsymbol{y}^{\text{true}}$ Vector of state variable true values.
Y_{ij} Element ij of the network admittance matrix, $\boldsymbol{Y}$.
G_{ij} Real part of Y_{ij}.
B_{ij} Imaginary part of Y_{ij}.
b_{ij}^s Total shunt susceptance of the π equivalent model of the line connecting nodes i and j.

I. Sets

Ω_i Set of buses adjacent to bus i.
Ω_0 Set of transit nodes associated with zero injections.
Ω_V Set of buses with available voltage magnitude measurements.
Ω_{P_c} Sets of buses with available active power injection measurements, where subindex $c = g, d, b$ refers to only generation, only demand and both.
Ω_{Q_c} Sets of buses with available reactive power injection measurements, where subindex $c = g, d, b$ refers to only generation, only demand and both.
Ω_{P_F} Set of lines with available active power flow measurements.
Ω_{Q_F} Set of lines with available reactive power flow measurements.
Ω_I Set of active inequality constraints.

J. Numbers

n Number of variables.
n_s Number of state variables.
m Number of measurements.
l Number of equality constraints.

p Number of the elements of data vector $\boldsymbol{a}$.
r Number of inequality constraints.
r_{Ω_I} Cardinality of Ω_I, i.e., the number of active inequality constraints.

K. Indices

i, j, k Indices used for buses, lines, and equality and inequality constraints.

L. Operators

∇_x Gradient or Jacobian with respect to x.
∇_{xx} Hessian with respect to x.
∇_{xa} Hessian with respect to x and a.

It should be noted that a variable, function or parameter written in bold without index is a vector form representing the corresponding quantities. For example, the symbol $\boldsymbol{\theta}$ represents the vector of bus voltage angles.

I. Introduction

A. Motivation

Owing to the complexities of operating large, interconnected networks, electric companies use modern Energy Management System (EMS). The purpose of an EMS is to monitor, control, and optimize the transmission and generation facilities with advanced computer technologies. The aim of the state estimation (SE) function is to obtain the best estimate of the current system state processing a set of real-time redundant measurements and network parameters available in the EMS database. The performance of the state estimator, therefore, depends on the accuracy of the measurements as well as on the parameters of the network model. The measurements are subject to noise or errors in the metering system and the communication process. Network parameters such as impedances or shunt susceptances of transmission lines may be incorrect as a result of inaccurate manufacturing provided data, errors in calibration, etc. In addition, due to the potential lack of field information, transformer tap positions may be erroneous. All these types of errors can severely impact the quality of the estimate provided by the state estimator. Thus, a fundamental question arises: How the estimation changes as measurements and parameters change? Answering rigorously this question is the subject and novel contribution of this paper.

B. Aim

We analyze changes in the estimated state variables and the estimation error with respect to different constants, such as measurements, measurement weights and network parameters. Changes in the state estimation as data marginally vary provide insight on the characteristics of the estimate of the current system state. This analysis is useful to assess the relevance for the estimation of each constant (measurement, measurement weight or parameter). However, note that sensitivities provide information for small changes, not for large changes.

C. Literature review

The problem of sensitivity analysis in nonlinear programming has been discussed by several authors, as, for example, [1]-[4]. In the derivations below, we use results reported in [2] and [4], based on differentiation of the Karush-Kuhn-Tucker conditions.

Concerning state estimation, pioneering paper [5], published in the seventies, clearly defines the problem addressed in this paper and points out its relevance. However, the proposed approach is based on numerical finite differences and therefore its scope is rather limited with respect to the technique advocated in this paper. The trajectory sensitivity analysis [6] is laterally related with the methodology proposed in this paper as well as paper [7] that addresses sensitivities of the residuals with respect to branch flows.

An application of sensitivity analysis within the context of an optimal power flow is carried out in [8]. The work in [8] provides a sensitivity analysis of market clearing prices (dual variables) with respect to economical constants and parameters using the sensitivity methodology described in [2] and [4]. The methodology developed in this paper applies the same sensitivity methodology as [8] but to a quite different problem: state estimation; particularly, it derives and discuss sensitivities of the error (objective function) and optimal estimates (primal variables) with respect to physical constants. Some preliminary results on state estimation sensitivity can be found in [9].

Background on state estimation can be found, for instance, in [10] and [11].

D. Paper organization

This paper is organized as follows. Section II provides the considered state estimation formulation. Section III presents the analytical expression used to compute the sensitivities. Section IV gives results from an illustrative example to demonstrate the functioning of the expressions derived. Section V gives results from a case study based on the IEEE Reliability Test System [12]. Section VI provides some relevant conclusions.

II. State Estimation Formulation

Consider the nonlinear measurement model:

$$\boldsymbol{z} = \boldsymbol{h}(\boldsymbol{y}^{\mathrm{true}}) + \boldsymbol{e}, \tag{1}$$

where $\boldsymbol{z}$ is the vector of measurements, $\boldsymbol{y}^{\mathrm{true}}$ is the true state vector, $\boldsymbol{h}$ is a nonlinear function vector relating measurements to states, and $\boldsymbol{e}$ is the measurement error vector. There are m measurements and n_s state variables, $n_s < m$.

In general, the state estimation problem can be formulated as an optimization problem including equality and inequality constraints as:

$$\underset{\boldsymbol{x}}{\text{minimize}} \quad J(\boldsymbol{x}, \boldsymbol{a}) \ \text{ subject to} \left\{ \begin{array}{lcl} \boldsymbol{c}(\boldsymbol{x}, \boldsymbol{a}) & = & \mathbf{0} : \boldsymbol{\lambda} \\ \boldsymbol{g}(\boldsymbol{x}, \boldsymbol{a}) & \leq & \mathbf{0} : \boldsymbol{\mu}, \end{array} \right. \tag{2}$$

where $\boldsymbol{x} \in \mathbb{R}^n$, $\boldsymbol{a} \in \mathbb{R}^p$, $J(\boldsymbol{x})$ is a scalar function of the estimation error, $\boldsymbol{c}(\boldsymbol{x}, \boldsymbol{a}) = (c_1(\boldsymbol{x}, \boldsymbol{a}), \ldots, c_\ell(\boldsymbol{x}, \boldsymbol{a}))^T$ are the equality constraints representing *exact pseudo-measurements* (zero injections) and power flow quantities (dependent variables), $\boldsymbol{g}(\boldsymbol{x},\boldsymbol{a}) = (g_1(\boldsymbol{x},\boldsymbol{a}),\ldots,g_r(\boldsymbol{x},\boldsymbol{a}))^T$ are inequality constraints normally used to represent physical operating limits in the network, and $\boldsymbol{\lambda}$ and $\boldsymbol{\mu}$ are the Lagrange multiplier vectors for equality and inequality constraints, respectively.

Note that nodal voltages and angles are considered as state variables. Power flows in branches are dependent variables and can be determined from the state variables.

For the derivation of the proposed state estimation sensitivity analysis, the weighted least squares (WLS) error with its associated hypothesis [13] is considered as the objective function. We use this objective function for illustration purposes. However, different objective functions including more robust estimators could be used and the method to be presented would remain valid. The only condition for this method to be applied is that the problem has to be stated as an optimization problem, and its solution must hold the KKT conditions [14].

The weighted measurement quadratic error function is:

$$\begin{aligned} J(\boldsymbol{x},\boldsymbol{a}) &= \sum_{i\in\Omega_V} w_i^V (v_i^m - v_i)^2 \\ &+\sum_{i\in\Omega_{P_c}} w_i^P (P_i^m - P_i)^2 + \sum_{i\in\Omega_{Q_c}} w_i^Q (Q_i^m - Q_i)^2 \\ &+ \sum_{(i,j)\in\Omega_{P_F}} w_{ij}^P (P_{ij}^m - P_{ij})^2 + \sum_{(i,j)\in\Omega_{Q_F}} w_{ij}^Q (Q_{ij}^m - Q_{ij})^2. \end{aligned} \tag{3}$$

Active and reactive power injections and flows are included as equality constraints:

$$\begin{aligned} P_i &= v_i \sum_{j\in\Omega_i} v_j \left(G_{ij}\cos(\theta_i-\theta_j) + B_{ij}\sin(\theta_i-\theta_j)\right), \\ & \quad i \in \{\Omega_{P_g}\cup\Omega_{P_d}\cup\Omega_{P_b}\cup\Omega_0\}. && (4)\\ Q_i &= v_i \sum_{j\in\Omega_i} v_j \left(G_{ij}\sin(\theta_i-\theta_j) - B_{ij}\cos(\theta_i-\theta_j)\right), \\ & \quad i \in \{\Omega_{P_g}\cup\Omega_{P_d}\cup\Omega_{P_b}\cup\Omega_0\}. && (5)\\ P_{ij} &= v_i v_j (G_{ij}\cos(\theta_i-\theta_j) + B_{ij}\sin(\theta_i-\theta_j)) \\ & \quad -G_{ij}v_i^2,\ (i,j)\in\Omega_{P_F}. && (6)\\ Q_{ij} &= v_i v_j (G_{ij}\sin(\theta_i-\theta_j) - B_{ij}\cos(\theta_i-\theta_j)) \\ & \quad +v_i^2(B_{ij} - b_{ij}^s/2),\ (i,j)\in\Omega_{Q_F}. && (7) \end{aligned}$$

For the sake of simplicity shunt elements are not considered in (4)-(7).

Virtual measurements are modeled as explicit constraints in the estimation problem as $P_i = 0$ and $Q_i = 0$, $i \in \Omega_0$.

Additionally, physical limits, such as minimum and maximum reactive power generation and angle extreme values, can also be enforced as inequality constraints to improve the representation:

$$\begin{aligned} P_i^{\min} &\le P_i \le P_i^{\max},\ i\in\Omega_{P_g} && (8)\\ Q_i^{\min} &\le Q_i \le Q_i^{\max},\ i\in\Omega_{P_g} && (9)\\ \boldsymbol{\theta}^{\min} &\le \boldsymbol{\theta} \le \boldsymbol{\theta}^{\max}, && (10) \end{aligned}$$

where constraints (8), (9) and (10) are bounds on active power injections, reactive power injections, and voltage angles, respectively. Usually, the angle extreme values are taken as $(-\pi,+\pi)$.

Note that vector $\boldsymbol{x}$ includes all variables ($\boldsymbol{v}$, $\boldsymbol{\theta}$, $\boldsymbol{P}$, $\boldsymbol{Q}$, $\boldsymbol{P}_F$, $\boldsymbol{Q}_F$) and vector $\boldsymbol{a}$ could include all data ($\boldsymbol{w}^V$, $\boldsymbol{v}^m$, $\boldsymbol{w}^P$, $\boldsymbol{P}^m$, $\boldsymbol{w}^Q$, $\boldsymbol{Q}^m$, $\boldsymbol{w}^{P_F}$, $\boldsymbol{P}_F^m$, $\boldsymbol{w}^{Q_F}$, $\boldsymbol{Q}_F^m$, $\boldsymbol{G}$, $\boldsymbol{B}$, $\boldsymbol{b}^s$, $\boldsymbol{P}^{\max}$, $\boldsymbol{P}^{\min}$, $\boldsymbol{Q}^{\max}$, $\boldsymbol{Q}^{\min}$, $\boldsymbol{\theta}^{\min}$, $\boldsymbol{\theta}^{\max}$). Note that the subscript F indicates flow quantity. Equality constraints include (4)-(7) and inequality constraints (8)-(10).

Considering the above formulation it is possible to evaluate the derivatives:

$$\begin{aligned} &\frac{\partial P_i}{\partial \boldsymbol{a}}; i\in\Omega^P, && \frac{\partial Q_i}{\partial \boldsymbol{a}}, i\in\Omega^Q, \\ &\frac{\partial P_{ij}}{\partial \boldsymbol{a}}; (i,j)\in\Omega_{P_F}, && \frac{\partial Q_{ij}}{\partial \boldsymbol{a}}, (i,j)\in\Omega_{Q_F}. \end{aligned} \tag{11}$$

In general, we develop analytical expressions to compute the sensitivities $\frac{\partial \boldsymbol{J}}{\partial \boldsymbol{a}}$ and $\frac{\partial \boldsymbol{x}}{\partial \boldsymbol{a}}$, that is, the sensitivities of the estimation error and the estimates with respect to the data, respectively. Nevertheless, any other sensitivity can be obtained using the procedure described in Section III.

III. General Sensitivity Expressions

A. Optimality Conditions

Considering appropriate regularity assumption[1] (see [14] or [15]) on problem (3)-(10) at its optimal solution $(\boldsymbol{x}^e, \boldsymbol{\lambda}^*, \boldsymbol{\mu}^*, J^*)$, the Karush-Kuhn-Tucker (KKT) first order optimality conditions are:

$$\begin{aligned} \nabla_{\boldsymbol{x}} J(\boldsymbol{x}^e,\boldsymbol{a}) + \sum_{k=1}^{\ell} \lambda_k^*\ \nabla_{\boldsymbol{x}} c_k(\boldsymbol{x}^e,\boldsymbol{a}) \\ + \sum_{j=1}^{r} \mu_j^*\ \nabla_{\boldsymbol{x}} g_j(\boldsymbol{x}^e,\boldsymbol{a}) = \boldsymbol{0} && (12)\\ c_k(\boldsymbol{x}^e,\boldsymbol{a}) = 0,\ \ k=1,2,\ldots,\ell && (13)\\ g_j(\boldsymbol{x}^e,\boldsymbol{a}) \le 0,\ \ j=1,2,\ldots,r && (14)\\ \mu_j^*\ g_j(\boldsymbol{x}^e,\boldsymbol{a}) = 0,\ \ j=1,2,\ldots,r && (15)\\ \mu_j^* \ge 0,\ \ j=1,2,\ldots,r\ . && (16) \end{aligned}$$

Conditions (13)-(14) are *the primal feasibility* conditions, conditions (15) are the *complementary slackness conditions*, and conditions (16) impose the nonnegativity of the multipliers of the inequality constraints, and are referred to as the *dual feasibility conditions*.

Unlike common practice in state estimation, the proposed algorithm is directly based on solving an optimization problem. We advocate this approach due to the versatility, efficiency and robustness of currently available optimization software. We emphasize that the available optimization codes efficiently account for sparsity and possible numerical ill-conditioning. Nevertheless, the solution of the estimation problem could be obtained using any of the available direct methods in the literature [13]. As the proposed sensitivity analysis needs information about the dual problem, the only previous step to the sensitivity study is to obtain the dual variables solving the linear system of equations constituted by equations (12), (15) and (16). If regularity conditions hold the solution of this system of equations is unique.

[1]For a given optimization problem, regularity entails that the gradient vectors of the binding constraints at a solution are linearly independent.

B. Feasible Perturbation

To obtain sensitivity equations, we perturb or modify $\boldsymbol{x}^e$, $\boldsymbol{a}$, $\boldsymbol{\lambda}^*$, $\boldsymbol{\mu}^*$, J^* in such a way that the KKT conditions still hold [4]. Thus, to obtain the sensitivity equations we differentiate the objective function $J(\boldsymbol{x}, \boldsymbol{a})$ and the optimality conditions (12)-(16), as follows:

$$[\nabla_{\boldsymbol{x}} J(\boldsymbol{x}^e, \boldsymbol{a})]^T d\boldsymbol{x} + [\nabla_{\boldsymbol{a}} J(\boldsymbol{x}^e, \boldsymbol{a})]^T d\boldsymbol{a} - dJ = 0 \quad (17)$$

$$\left[\nabla_{\boldsymbol{xx}} J(\boldsymbol{x}^e, \boldsymbol{a}) + \sum_{k=1}^{\ell} \lambda_k^* \nabla_{\boldsymbol{xx}} c_k(\boldsymbol{x}^e, \boldsymbol{a}) + \sum_{j=1}^{r_{\Omega_I}} \mu_j^* \nabla_{\boldsymbol{xx}} g_j(\boldsymbol{x}^e, \boldsymbol{a})\right] d\boldsymbol{x} + \left[\nabla_{\boldsymbol{xa}} J(\boldsymbol{x}^e, \boldsymbol{a}) + \sum_{k=1}^{\ell} \lambda_k^* \nabla_{\boldsymbol{xa}} c_k(\boldsymbol{x}^e, \boldsymbol{a}) + \sum_{j=1}^{r_{\Omega_I}} \mu_j^* \nabla_{\boldsymbol{xa}} g_j(\boldsymbol{x}^e, \boldsymbol{a})\right] d\boldsymbol{a} + \nabla_{\boldsymbol{x}} \boldsymbol{c}(\boldsymbol{x}^e, \boldsymbol{a}) d\boldsymbol{\lambda} + \nabla_{\boldsymbol{x}} \boldsymbol{g}(\boldsymbol{x}^e, \boldsymbol{a}) d\boldsymbol{\mu} = \boldsymbol{0} \quad (18)$$

$$[\nabla_{\boldsymbol{x}} \boldsymbol{c}(\boldsymbol{x}^e, \boldsymbol{a})]^T d\boldsymbol{x} + [\nabla_{\boldsymbol{a}} \boldsymbol{c}(\boldsymbol{x}^e, \boldsymbol{a})]^T d\boldsymbol{a} = \boldsymbol{0} \quad (19)$$

$$[\nabla_{\boldsymbol{x}} g_j(\boldsymbol{x}^e, \boldsymbol{a})]^T d\boldsymbol{x} + [\nabla_{\boldsymbol{a}} g_j(\boldsymbol{x}^e, \boldsymbol{a})]^T d\boldsymbol{a} = 0 \quad \text{if } \mu_j^* \neq 0, j \in \Omega_I \;, \quad (20)$$

where all the matrices are evaluated at the optimal solution, $\boldsymbol{x}^e$, $\boldsymbol{\lambda}^*$, $\boldsymbol{\mu}^*$, J^*. It should be noted that the derivation above is based on results reported in [4].

Once an optimal solution of the estimation problem is known, binding inequality constraints are considered equality constraints and non-binding ones are disregarded. Note that this is appropriate as our analysis is just local. We assume local convexity around an optimal solution, which might not imply a globally optimal solution. Note also that inequality constraints (8)-(10) have generally a small influence in the solution of the state estimation problems and the associated sensitivities as equality constraints (4)-(7) tightly condition that solution. Inequality constraints merely enforce that physical limits are not slightly violated and therefore they can be included or not in the formulation.

Considering binding inequality constraints as equality constraints, the linear system of equations (17)-(20) can be expressed in matrix form as follows:

$$\left[\begin{array}{c|c|c|c} \boldsymbol{F_x} & \boldsymbol{F_a} & \boldsymbol{0} & -1 \\ \hline \boldsymbol{F_{xx}} & \boldsymbol{F_{xa}} & \boldsymbol{C_x^T} & 0 \\ \hline \boldsymbol{C_x} & \boldsymbol{C_a} & \boldsymbol{0} & 0 \end{array}\right] \left[\begin{array}{c} d\boldsymbol{x} \\ d\boldsymbol{a} \\ d\boldsymbol{\lambda} \\ dJ \end{array}\right] = \boldsymbol{0}, \quad (21)$$

where the vectors and submatrices in (21) are defined in Appendix I.

C. Sensitivity Expressions

To compute sensitivities with respect to the components of the data vector $\boldsymbol{a}$, system (21) can be written as

$$\boldsymbol{U} \left[\ d\boldsymbol{x} \quad d\boldsymbol{\lambda} \quad dJ\ \right]^T = \boldsymbol{S}\, d\boldsymbol{a}\ , \quad (22)$$

where the matrices $\boldsymbol{U}$ and $\boldsymbol{S}$ are

$$\boldsymbol{U} = \left[\begin{array}{c|c|c} \boldsymbol{F_x} & \boldsymbol{0} & -1 \\ \hline \boldsymbol{F_{xx}} & \boldsymbol{C_x^T} & 0 \\ \hline \boldsymbol{C_x} & \boldsymbol{0} & 0 \end{array}\right] \quad (23)$$

$$\boldsymbol{S}^T = -\left[\ \boldsymbol{F_a} \quad \boldsymbol{F_{xa}} \quad \boldsymbol{C_a}\ \right] \quad (24)$$

and therefore

$$\left[\ d\boldsymbol{x} \quad d\boldsymbol{\lambda} \quad dJ\ \right]^T = \boldsymbol{U}^{-1} \boldsymbol{S}\, d\boldsymbol{a}\ . \quad (25)$$

Replacing $d\boldsymbol{a}$ by the p-dimensional identity matrix $\boldsymbol{I}$ in (25) the matrix with all derivatives with respect to data is obtained

$$\left[\ \frac{\partial \boldsymbol{x}}{\partial \boldsymbol{a}} \quad \frac{\partial \boldsymbol{\lambda}}{\partial \boldsymbol{a}} \quad \frac{\partial J}{\partial \boldsymbol{a}}\ \right]^T = \boldsymbol{U}^{-1} \boldsymbol{S}\ . \quad (26)$$

Expression (26) allows deriving sensitivities of the variables, the multipliers (dual variables) and the objective function with respect to all parameters.

Considering matrices

$$\boldsymbol{H}_x = \left[\begin{array}{c|c} \boldsymbol{F_{xx}} & \boldsymbol{C_x^T} \\ \hline \boldsymbol{C_x} & \boldsymbol{0} \end{array}\right] \text{ and } \boldsymbol{H}_a = \left[\begin{array}{c} \boldsymbol{F_{xa}} \\ \hline \boldsymbol{C_a} \end{array}\right],$$

where $\boldsymbol{H}_x$ is symmetrical, expression (26) can be solved as follows:

$$\left[\frac{\partial \boldsymbol{x}}{\partial \boldsymbol{a}}\ \frac{\partial \boldsymbol{\lambda}}{\partial \boldsymbol{a}}\right]^T = -\boldsymbol{H}_{\boldsymbol{x}}^{-1} \boldsymbol{H_a} \quad (27)$$

$$\frac{\partial J}{\partial \boldsymbol{a}} = \boldsymbol{F_a} + \boldsymbol{F_x} \frac{\partial \boldsymbol{x}}{\partial \boldsymbol{a}}. \quad (28)$$

It should be noted that matrices $\boldsymbol{U}$ and $\boldsymbol{H}_x$ are generally invertible as power flow equations (4)-(7) and binding physical limits (8)-(10) are regular, non-degenerated constraints. Moreover, extensive numerical experiments show a good numerical behaviour of matrices $\boldsymbol{U}$ and $\boldsymbol{H}_x$ for the state estimation problem, provided that the state is observable and regardless of the number of measurements. Note also that matrices $\boldsymbol{U}$ and $\boldsymbol{H}_x$ are highly sparse as a result of the sparsity of its building blocks (see (23)) and it is easily factorized using sparse-oriented LU algorithms.

IV. Illustrative Example

A. Description

The 6-bus power system depicted in Fig. 1 is considered in this section [16]. The data for this system is provided in Appendix II.

The measurement configuration shown in Fig. 1 provides a measurement redundancy ratio of 1.82 (measurements are given in Appendix II). Measurements are synthetically generated by adding randomly generated gaussian errors to the true values.

For simplicity, only two different values for the standard deviations of the measurements are used: 0.01 for voltage measurements and 0.02 for flow and injection measurements. These values correspond to weights of 10000 and 2500, respectively.

This example includes generating buses ($\Omega_{P_g} = \{1, 2, 3\}$), demand buses ($\Omega_{P_d} = \{4, 5, 6\}$), but no transit buses ($\Omega_0 = \emptyset$).

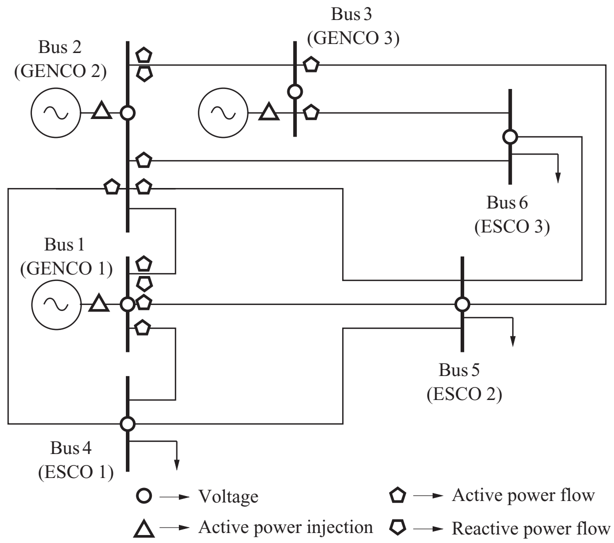

Fig. 1. Six-bus system and available meters.

The WLS state estimation problem (3)-(10) is solved for this example and the results obtained reported and discussed below.

The optimal error provided by the state estimator is $J(\boldsymbol{x}^e) \approx 8.71$ holding the χ^2-test for bad data detection with a confidence probability of 95%: $J(\boldsymbol{x}^e) < \chi^2_{9,0.95} \Longrightarrow 8.13 < 16.92$. Table I provides the measurements, the true values and the estimates of the state variables.

TABLE I

OPTIMAL ESTIMATION SOLUTION

Bus #	v_i^m (p.u.)	v_i^{true} (p.u.)	v_i^e (p.u.)	θ_i^{true} (rad)	θ_i^e (rad)
1	1.097	1.100	1.095	0.000	0.000
2	1.103	1.100	1.096	-0.047	-0.047
3	1.102	1.098	1.094	-0.091	-0.094
4	1.000	1.018	1.014	-0.090	-0.090
5	0.999	1.006	0.999	-0.121	-0.123
6	1.024	1.034	1.029	-0.128	-0.130

B. Sensitivities of the estimation error

1) Sensitivities of the estimation error with respect to voltage measurements and active power injection measurements, respectively, are provided in the matrix below (units are $1/\mathrm{puV}$ and $1/\mathrm{puMW}$, respectively):

$$\left[\frac{\partial J^*}{\partial v_i^m}\,\frac{\partial J^*}{\partial P_i^m}\right] = \begin{bmatrix} -83.51686 & 13.74085 \\ 52.56376 & 37.94881 \\ 182.90047 & -75.92968 \\ -61.89823 & - \\ -71.10769 & - \\ -9.10143 & - \end{bmatrix},$$

where subscript i refers to rows (buses) and the symbol "$-$" means that the corresponding measurement does not exist. Note also that these results coincide with the ones obtained using the analytical expressions:

$$\frac{\partial J(\boldsymbol{x})}{\partial v_i^m} \;=\; 2w_i^V(v_i^m - v_i);\; i \in \Omega_V, \qquad (29)$$

and the analogous ones for the active power injection.

The observations below are pertinent: a) The estimation error is more sensitive to voltage measurements than to power injection measurements. This is in accordance with the hypothesis that establishes a smaller standard deviation for voltage measurements. b) The highest sensitivities are associated with bus 3. This fact is not obvious and demonstrates the added value of the proposed analysis, which allows us to better comprehend estimation results.

It should be noted that in order to compare sensitivities with respect to different parameters the normalized sensitivity $|x_i|\frac{\partial J}{\partial x_i}$ should be used.

2) Sensitivities of the estimation error with respect to active and reactive power flow measurements are shown in the matrix below (units are $1/\mathrm{puMW}$ and $1/\mathrm{puMVAr}$, respectively):

$$\left[\frac{\partial J^*}{\partial P_{ij}^m}\,\frac{\partial J^*}{\partial Q_{ij}^m}\right] = \begin{array}{c} \begin{bmatrix} 1.22457 & 21.12468 \\ 26.45085 & - \\ -31.01097 & - \\ -51.48155 & 3.97837 \\ -61.60584 & - \\ 115.68962 & - \\ -55.78377 & - \\ -195.836 & - \\ -57.27579 & - \end{bmatrix} \end{array} \begin{array}{c} (1,2) \\ (1,4) \\ (1,5) \\ (2,3) \\ (2,4) \\ (2,5) \\ (2,6) \\ (3,5) \\ (3,6) \end{array}.$$

Parentheses on the right hand side of the matrix represent lines. Observe that the sensitivities with respect to active power flow measurements in lines connected to bus 5 present high absolute values, which leads to the (non obvious) conclusion that the measurements related to bus 5 play a critical role in the estimation.

Note that these results coincide with the ones obtained using the analytical expressions:

$$\frac{\partial J(\boldsymbol{x})}{\partial P_{ij}^m} \;=\; 2w_i^{P_F}(P_{ij}^m - P_{ij});\; (i,j) \in \Omega_{P_F} \qquad (30)$$

and the analogous ones for the reactive power flow measurements.

3) Sensitivity of the estimation error with respect to the reactances and shunt susceptances of the lines are provided below (units are $1/\mathrm{pu}\Omega$ and $1/\mathrm{puS}$, respectively):

$$\left[\frac{\partial J^*}{\partial x_{ij}}\,\frac{\partial J^*}{\partial b_{ij}^s}\right] = \begin{bmatrix} -33.4275 & 12.8047 \\ 125.9441 & 0 \\ -31.6880 & 0 \\ -61.2126 & 2.4082 \\ -208.6190 & 0 \\ 207.1907 & 0 \\ -48.6960 & 0 \\ -160.6123 & 0 \\ 53.7817 & 0 \\ 0 & 0 \\ 0 & 0 \end{bmatrix} \begin{array}{c} (1,2) \\ (1,4) \\ (1,5) \\ (2,3) \\ (2,4) \\ (2,5) \\ (2,6) \\ (3,5) \\ (3,6) \\ (4,5) \\ (5,6) \end{array}.$$

Sensitivities with respect to line reactances and shunt susceptances are obtained from sensitivities with respect to the elements of the admittance matrix ($\boldsymbol{Y}$) using the chain rule as stated in Appendix III. Note the significant dependency of the estimation error with respect to reactances $x_{2,4}$ and $x_{2,5}$. Note the these reactances are related to bus 2. Note also that the sensitivities with respect to reactances x_{45} and x_{56} are zero because the objective function does not include flow measurements pertaining to lines $(4,5)$ and $(5,6)$ and therefore reactances $x_{4,5}$ and $x_{5,6}$ appear neither in the objective function nor in the constraints of the estimation problem.

4) Sensitivities of the estimation error with respect to power injection lower bounds are provided in the vector below (units are $1/\mathrm{puMW}$)

$$\left[\frac{\partial J^*}{dP_i^{\min}}\right]^T = \left[\begin{array}{ccc} 0 & 0 & 141.6671 \end{array}\right];\; i \in \Omega_{P_g}.$$

Note that the first two elements are zero because the estimated (active power) generations for the generators in buses 1 and 2 are between their respective bounds, whereas for the generator in bus 3 the sensitivity is different from zero because the estimate of the (active power) generation equals its lower bound.

5) Analytical expressions to compute the sensitivities of the error function with respect to weights are available. For the voltage measurement weights the expressions are:

$$\frac{\partial J(\boldsymbol{x})}{\partial w_i^V} \;=\; (v_i^m - v_i)^2;\; i \in \Omega_V. \tag{31}$$

Analogous expressions exist for the remaining weights. Note that results obtained by (31) coincide with the ones provided by the proposed method.

C. Sensitivities of voltage estimates

1) Sensitivities of the voltage estimates with respect to the voltage measurements are shown below:

$$\left[\frac{\partial v_i^e}{\partial v_j^m}\right] = \begin{bmatrix} 0.39803 & 0.29362 & 0.23857 & 0.04877 & 0.00866 & 0.01503 \\ 0.29362 & 0.32345 & 0.26178 & 0.07214 & 0.02217 & 0.01842 \\ 0.23857 & 0.26178 & 0.37505 & 0.05458 & 0.04309 & 0.01083 \\ 0.04877 & 0.07214 & 0.05458 & 0.79484 & 0.03464 & 0.00814 \\ 0.00866 & 0.02217 & 0.04309 & 0.03464 & 0.91172 & -0.01697 \\ 0.01503 & 0.01842 & 0.01083 & 0.00814 & -0.01697 & 0.96873 \end{bmatrix},$$

where subscript i refers to rows while subscript j refers to columns. The following observations are pertinent: a) the matrix is dimensionless, symmetric and diagonally dominant, and b) it is full as all voltage estimates change as any voltage measurement change occurs. Numerical experiments show that the matrix above becomes less diagonal dominant as the number of measurements increases.

2) Sensitivities of the voltage estimate in bus 4 (a load bus) with respect to active and reactive power injection measurements are provided below (units are $\mathrm{puV/puMW}$ and $\mathrm{puV/puMVAr}$, respectively):

$$\left[\frac{\partial v_4^e}{\partial P_{ij}^m}\;\frac{\partial v_4^e}{\partial Q_{ij}^m}\right] = \begin{array}{c} \begin{bmatrix} -0.08763 & 0.00670 \\ 0.13440 & - \\ -0.04860 & - \\ -0.00011 & 0.01836 \\ -0.09036 & - \\ 0.01499 & - \\ 0.00362 & - \\ 0.01592 & - \\ -0.01596 & - \end{bmatrix} \end{array} \begin{array}{c} (1,2) \\ (1,4) \\ (1,5) \\ (2,3) \\ (2,4) \\ (2,5) \\ (2,6) \\ (3,5) \\ (3,6) \end{array}.$$

Lines are indicated in parentheses at the right hand side of the matrix.

Observe that the highest sensitivity corresponds to the active power flow measurement (1,4). Note also the significant influence of the reactive power flow measurement (2,3).

3) Sensitivities of the voltage estimates with respect to active power injection measurements are provided below (units are $\mathrm{puV/puMW}$):

$$\left[\frac{\partial v_i^e}{\partial P_j^m}\right] = \begin{bmatrix} 0.01067 & -0.00867 & 0 \\ -0.00697 & 0.00195 & 0 \\ -0.00766 & -0.00249 & 0 \\ -0.00183 & 0.01219 & 0 \\ 0.00537 & -0.00295 & 0 \\ 0.00020 & -0.00109 & 0 \end{bmatrix},\; i \in \Omega_{P_g},$$

where subscript i refers to rows and subscript j refers to columns.

It should be noted that the sensitivities of all voltage estimates with respect to the power injection measurement in bus 3 are zero because the estimate of the power injection in that bus is equal to its lower limit.

4) Sensitivities of the voltage estimates with respect to line reactances are provided below (units are $\mathrm{puV/pu\Omega}$):

$$\left[\frac{\partial v_i^e}{\partial x_{jk}}\right]^T = \begin{bmatrix} -0.039 & 0.080 & 0.070 & -0.080 & -0.025 & 0.001 \\ -0.101 & -0.146 & -0.110 & 0.420 & -0.070 & -0.016 \\ 0.007 & -0.030 & -0.048 & -0.093 & 0.146 & 0.018 \\ -0.018 & -0.019 & 0.018 & -0.000 & -0.024 & 0.040 \\ 0.177 & 0.254 & 0.193 & -0.729 & 0.117 & 0.028 \\ -0.035 & -0.021 & -0.041 & 0.034 & 0.040 & 0.017 \\ 0.082 & 0.010 & 0.060 & 0.044 & -0.092 & -0.175 \\ 0.031 & 0.044 & 0.081 & 0.032 & -0.154 & -0.028 \\ -0.090 & -0.109 & -0.066 & -0.048 & 0.100 & 0.192 \\ 0 & 0 & 0 & 0 & 0 & 0 \\ 0 & 0 & 0 & 0 & 0 & 0 \end{bmatrix} \begin{array}{c} (1,2) \\ (1,4) \\ (1,5) \\ (2,3) \\ (2,4) \\ (2,5) \\ (2,6) \\ (3,5) \\ (3,6) \\ (4,5) \\ (5,6) \end{array},$$

where subscript i refers to columns and lines are indicated in parentheses at the right hand side of the matrix.

Observe that for the last three buses, the highest absolute value sensitivity is associated with one of the lines connected to that bus, i.e., x_{24} for node 4, x_{35} for node 5, and x_{36} for node 6. However, for the first three buses, the highest absolute value sensitivity is associated with the reactance of line $(2,4)$.

Note also that the sensitivities of the voltage estimates with respect to the reactances of lines (4,5) and (5,6) are null because no measurement pertaining these lines are considered in the objective function and constraints of the estimation problem.

5) Sensitivities of the voltage estimates with respect to line shunt susceptances of lines $(1,2)$ and $(2,3)$ are (units are $\mathrm{puV/puS}$):

$$\left[\frac{\partial v_i^e}{\partial b_{jk}^s}\right]^T = \begin{bmatrix} 0.0656 & -0.0382 & -0.0314 & 0.0040 & 0.0001 & -0.0018 \\ 0.0344 & 0.0390 & -0.0779 & 0.0111 & -0.0098 & 0.0015 \end{bmatrix} \begin{array}{c} (1,2) \\ (2,3) \end{array}.$$

Note that these lines are selected because reactive power flow measurements are available for them. Sensitivities with respect to the remaining line shunt susceptances are null.

6) The sensitivities of the voltage estimates with respect to the active power injection lower bounds are shown in the matrix below (units are $\mathrm{puV/puMW}$):

$$\left[\frac{\partial v_i^e}{\partial P_j^{\min}}\right] = \begin{bmatrix} 0 & 0 & 0.00189 \\ 0 & 0 & 0.00720 \\ 0 & 0 & 0.01493 \\ 0 & 0 & 0.00846 \\ 0 & 0 & -0.01672 \\ 0 & 0 & -0.01467 \end{bmatrix},\; i \in \Omega_{P_g},$$

where i refers to rows and j to columns.

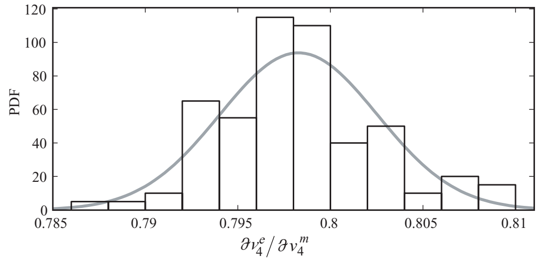

Fig. 2. Sensitivity $\partial v_4^e/\partial v_4^m$ histogram and normal PDF fit for the Illustrative Example with 100 simulations.

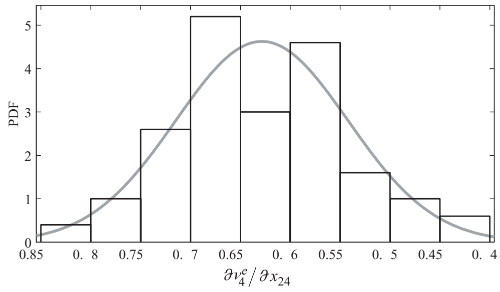

Fig. 3. Sensitivity $\partial v_4^e/\partial x_{24}$ histogram and normal PDF fit for the Illustrative Example with 100 simulations.

Bus 5 presents the highest absolute value sensitivity. Note also that generators 1 and 2 work at their (active power generation) lower bounds, being their corresponding sensitivities null.

7) Finally, it should be noted that all absolute value sensitivities of the voltage estimates with respect to measurement weights are lower than 10^{-5}.

D. Statistical Analysis

The proposed method allows obtaining the sensitivities pertaining to a given measurement scenario, the one that materializes. These sensitivities can be used to make on-line decisions. Nevertheless, different scenarios of measurements can be randomly generated and the sensitivities obtained for each measurement scenario used for off-line analysis. An example of statistical analysis is provided below.

For 100 different measurement scenarios, the sensitivities of the voltage estimate at bus 4 with respect to voltage measurement at that bus, the sensitivities of the voltage estimate at bus 4 with respect to the line reactance connecting buses 2 and 4, and the sensitivities of the voltage estimate at bus 1 with respect to line shunt susceptance of line $(1, 2)$, respectively, are obtained and an statistical analysis is performed. In Figs. 2, 3 and 4, respectively, the histograms and PDF fits for the three sensitivity distributions are shown.

Note that the behavior of each distribution is Gaussian. Note also that the mean values of the sensitivity distributions and the corresponding sensitivities obtained using the exact

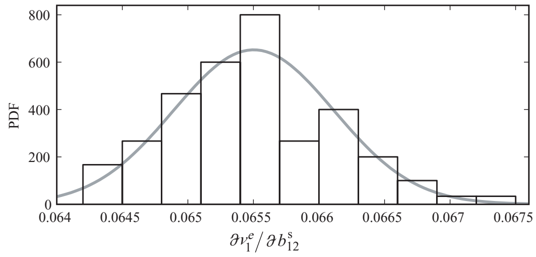

Fig. 4. Sensitivity $\partial v_1^e/\partial b_{12}^s$ histogram and normal PDF fit for the Illustrative Example with 100 simulations.

measurements are very similar, i.e.,

$$\begin{aligned} &\mathrm{E}\left\{\frac{\partial v_4^e}{\partial v_4^m}\right\} = 0.7983, && \left.\frac{\partial v_4^e}{\partial v_4^m}\right|_{\mathrm{tm}} = 0.7981 \\ &\mathrm{E}\left\{\frac{\partial v_4^e}{\partial x_{24}}\right\} = -0.6284, && \left.\frac{\partial v_4^e}{\partial x_{24}}\right|_{\mathrm{tm}} = -0.6267 \\ &\mathrm{E}\left\{\frac{\partial v_1^e}{\partial b_{12}^s}\right\} = 0.06546, && \left.\frac{\partial v_1^e}{\partial b_{12}^s}\right|_{\mathrm{tm}} = 0.06550. \end{aligned} \tag{32}$$

where $|_{\mathrm{tm}}$ indicates that measurements equal to the true values are used.

V. Case Study

A. Data

A case study based on the IEEE RTS, depicted in Fig. 5, is briefly presented and discussed in this section. Topology, generator and line data can be found in [12] (Fig. 1 and Tables 9 and 12, respectively, of that reference).

The measurement configuration shown in Fig. 5 provides a measurement redundancy ratio of 1.6. Measurements are synthetically generated by adding randomly generated errors to the true values.

The optimal error provided by the estimator is $J(\boldsymbol{x}^e) \approx 40.5$ holding the χ^2-test for bad data detection with a confidence probability of 95%: $J(\boldsymbol{x}^e) < \chi^2_{28,0.95} \Longrightarrow 40.5 < 41.34$.

In this case study the sets corresponding to zero injection, only generation, only demand, and both (generation and demand) are, respectively, $\Omega_0 = \{11, 12, 17, 24\}$, $\Omega_{P_g} = \{21, 22, 23\}$, $\Omega_{P_d} = \{3, 4, 5, 6, 8, 9, 10, 14, 19, 20\}$ and $\Omega_{P_b} = \{1, 2, 7, 13, 15, 16, 18\}$.

Standard deviation values for measurements are identical to those used in the example (Section IV). Note that in the buses with both generation and demand, the power injection is obtained as the difference between generation and demand. As the sum of two independent normal random variables is normal with a variance equal to the sum of the variances of the two random variables, the power injection weights related to generation plus demand buses are:

$$w_i^P = \frac{1}{(0.02)^2 + (0.02)^2} = 1250;\ i \in \Omega_{P_b}.$$

The sparse structure of matrices $\boldsymbol{U}$ and $\boldsymbol{H}_x$ for this case study is shown in Fig. 6. Matrix $\boldsymbol{H}_x$ is obtained deleting the first row and the last column of $\boldsymbol{U}$.

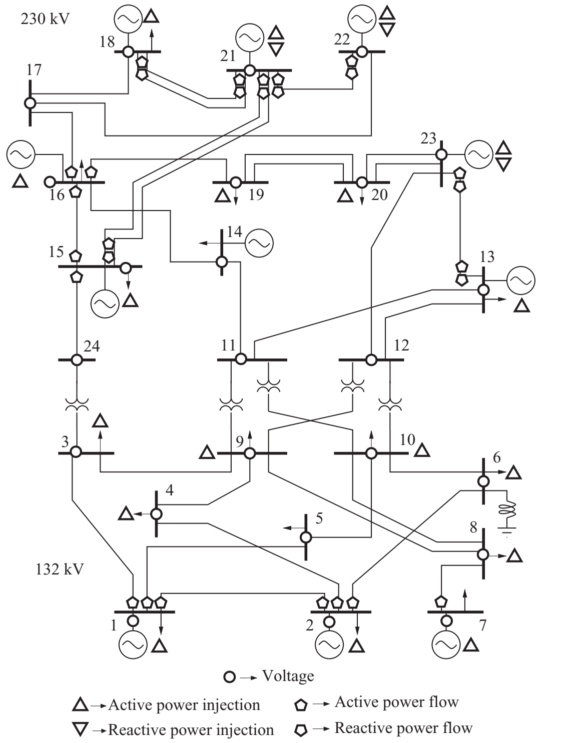

Fig. 5. IEEE 24-Bus Reliability Test System [12] and available meters in the system.

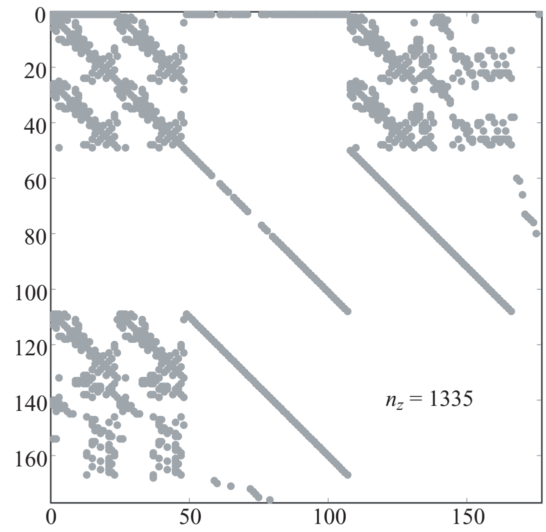

Fig. 6. Sparse structure of matrix $\boldsymbol{U}$ for the 24-bus test system. n_z is the number of nonzero elements.

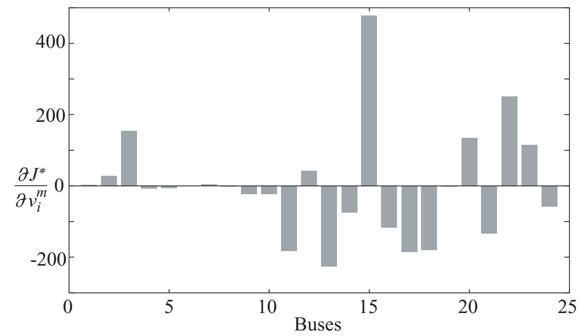

Fig. 7. Sensitivities $\partial J^*/\partial v_i^m$ for the 24-bus test system.

B. Results

A selection of the results obtained is described and discussed below.

1) Fig. 7 provides the sensitivities of the estimation error with respect to voltage measurements (units are $1/\mathrm{puV}$). Note that the highest sensitivities correspond to buses 15, 22 and 13. Positive sensitivities correspond to measurements higher than their corresponding estimates while negative ones to measurements lower than their corresponding estimates.

2) Sensitivity of the estimation error with respect to the line reactances and shunt susceptances are shown in Fig. 8 (units are $1/\mathrm{pu}\Omega$ and $1/\mathrm{puS}$, respectively). Note that each element in the abscissa axis is associated with a line using the following correspondence:

1	(1, 2)	2	(1, 3)	3	(1, 5)	4	(2, 4)	5	(2, 6)	6	(3, 9)
7	(3,24)	8	(4, 9)	9	(5,10)	10	(6,10)	11	(7, 8)	12	(8, 9)
13	(8,10)	14	(9,11)	15	(9,12)	16	(10,11)	17	(10,12)	18	(11,13)
19	(11,14)	20	(12,13)	21	(12,23)	22	(13,23)	23	(14,16)	24	(15,16)
25	(15,21)	26	(15,24)	27	(16,17)	28	(16,19)	29	(17,18)	30	(17,22)
31	(18,21)	32	(19,20)	33	(20,23)	34	(21,22)				

The highest sensitivities of the estimation error with respect to the reactance parameters correspond to lines $(15, 21)$, $(16, 17)$ and $(14, 16)$. The highest sensitivities of the estimation error with respect to the shunt susceptances correspond to lines $(19, 20)$, $(21, 22)$, $(13, 23)$ and $(15, 21)$. Note the different order of magnitudes of the sensitivities with respect to the reactances and the shunt susceptances, respectively.

3) Sensitivities of the voltage estimate at bus 11 (a transit node) with respect to voltage measurements are shown in Fig. 9 (dimensionless). The highest sensitivities correspond to measurements in buses 14 and 11, respectively. Note that generation bus 14 is directly connected to bus 11.

4) Sensitivities of the voltage estimate at bus 7 (a peripheral bus) with respect to active power flow measurements are shown in Fig. 10 (units are $\mathrm{puV}/\mathrm{puMW}$). Note that each element in the abscisas axis is associated with a line measurement using the following correspondence:

1	(1, 2)	2	(1, 3)	3	(1, 5)	4	(2, 4)	5	(2, 6)
6	(7, 8)	7	(13,23)	8	(15,16)	9	(15,21)	10	(15,24)
11	(16,17)	12	(16,19)	13	(18,21)	14	(21,22)	15	(2, 1)
16	(16,15)	17	(21,15)	18	(21,18)	19	(22,21)	20	(23,13)

As expected, the highest sensitivity corresponds to flow $(7, 8)$ because line (7,8) is connected to the network only through bus 8.

5) Sensitivities of the voltage estimates at bus 11 with respect to reactances and shunt susceptances of the lines are shown in Figs. 11 (a) and (b) (units are $\mathrm{puV}/\mathrm{pu}\Omega$ and $\mathrm{puV}/\mathrm{puS}$, respectively). Note that the highest values in Fig. 11 (a) correspond to the reactance of the lines $(15, 21)$, $(16, 17)$ and $(14, 16)$, whereas in Fig. 11 (b) correspond to line (13,23) and the lines adjacent to bus 11, which are equal.

6) Sensitivities of the active power flow estimate in line $(15, 16)$ (a typical line) with respect to the reactances of the

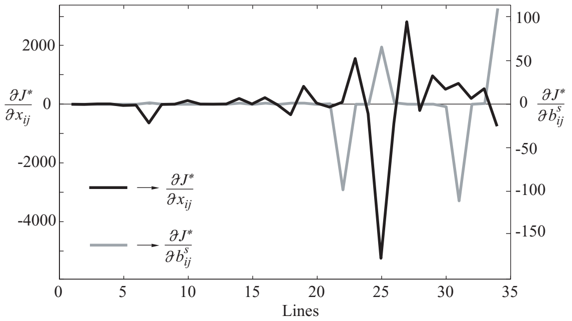

Fig. 8. Sensitivities $\partial J^*/\partial x_{ij}$ and $\partial J^*/\partial b^s_{ij}$ for the 24-bus test system.

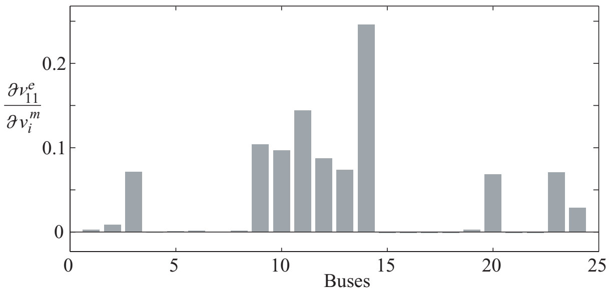

Fig. 9. Sensitivities $\partial v^e_{11}/\partial v^m_i$ for the 24-bus test system.

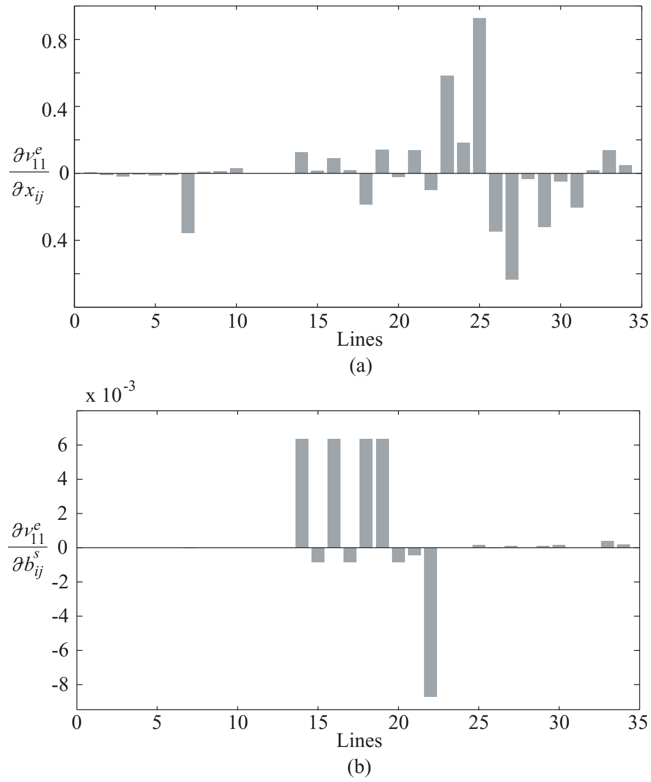

Fig. 11. Sensitivities (a) $\partial v^e_{11}/\partial x_{ij}$ and (b) $\partial v^e_{11}/\partial b^s_{ij}$ for the 24-bus test system.

lines are shown in Fig. 12 (units are $\mathrm{puMW/pu\Omega}$). Note that the highest sensitivities occur for lines (15,21), (16,17), (17,18) and (18,21), respectively.

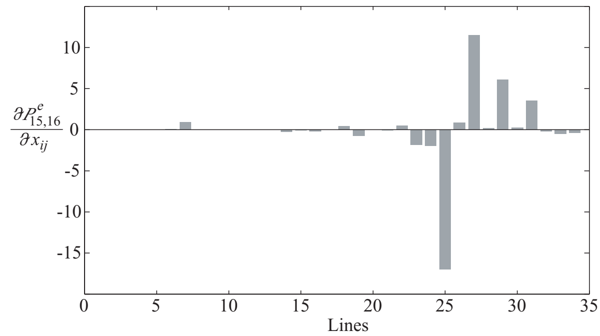

Fig. 12. Sensitivities $\partial P^e_{15,16}/\partial x_{ij}$ for the 24-bus test system.

VI. Conclusion

Within a state estimation framework, this paper provides simple analytical expressions to compute sensitivities of the estimation error and the estimates with respect to changes in measurements, bounds, weights and line parameters. The method is useful to increase the confidence in a state estimation model and its estimates. It has the following advantages: 1) the method provide information about the most influential measurements, and 2) it allows to know how important are the values of different parameters (measurements, weights, line parameters and bounds) in the estimation process.

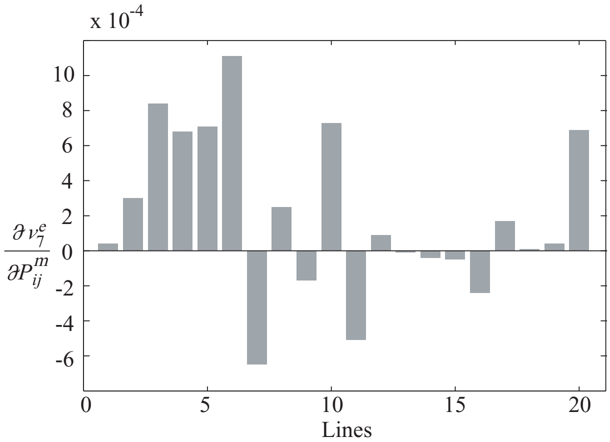

Fig. 10. Sensitivities $\partial v^e_7/\partial P^m_{ij}$ for the 24-bus test system.

An example and a case study are used to illustrate the sensitivity formulas derived. Extensive numerical simulation proved the validity and relevance of these sensitivity expressions, which have been validated through finite difference simulations.

It should be noted that calculating sensitivities of the estimation error and estimates with respect to transformer tap positions and topology changes constitute the subject of future work. Particularly, note that both tap positions and topology changes need to be modeled through discrete not continuous variables, which highly complicates a rigorous sensitivity analysis.

APPENDIX I
FEASIBLE PERTURBATION MATRICES

Vectors and submatrices in (21) required for obtaining the sensitivities are defined below (dimensions in parenthesis)

$$\boldsymbol{F}_{\boldsymbol{x}(1\times n)} = [\nabla_{\boldsymbol{x}} J(\boldsymbol{x}^e,\boldsymbol{a})]^T \tag{33}$$

$$\boldsymbol{F}_{\boldsymbol{a}(1\times p)} = (\nabla_{\boldsymbol{a}} J(\boldsymbol{x}^e,\boldsymbol{a}))^T \tag{34}$$

$$\boldsymbol{F}_{\boldsymbol{xx}(n\times n)} = \nabla_{\boldsymbol{xx}} J(\boldsymbol{x}^e,\boldsymbol{a}) + \sum_{k=1}^{\ell+r_{\Omega_I}} \lambda_k^* \nabla_{\boldsymbol{xx}} c_k(\boldsymbol{x}^e,\boldsymbol{a}) \tag{35}$$

$$\boldsymbol{F}_{\boldsymbol{xa}(n\times p)} = \nabla_{\boldsymbol{xa}} J(\boldsymbol{x}^e,\boldsymbol{a}) + \sum_{k=1}^{\ell+r_{\Omega_I}} \lambda_k^* \nabla_{\boldsymbol{xa}} c_k(\boldsymbol{x}^e,\boldsymbol{a}) \tag{36}$$

$$\boldsymbol{C}_{\boldsymbol{x}((\ell+r_{\Omega_I})\times n)} = [\nabla_{\boldsymbol{x}} \boldsymbol{c}(\boldsymbol{x}^e,\boldsymbol{a})]^T \tag{37}$$

$$\boldsymbol{C}_{\boldsymbol{a}((\ell+r_{\Omega_I})\times p)} = [\nabla_{\boldsymbol{a}} \boldsymbol{c}(\boldsymbol{x}^e,\boldsymbol{a})]^T. \tag{38}$$

APPENDIX II
DATA FOR THE SIX-BUS SYSTEM

Data are provided in Tables II, III and IV. Voltage magnitudes throughout the network should be between 1.1 and 0.9 p.u. No reactive power generating limits are considered. As it is customary, the considered three-phase power base is 100 MVA.

TABLE II
GENERATOR DATA AND RESULTS

Bus	$P_i^{\rm true}$	P_i^m	P_i^e	$P_i^{\max}$	$P_i^{\min}$
i	(p.u. MW)				
1	1.325	1.317	1.314	1.325	1.125
2	1.606	1.625	1.618	1.650	1.400
3	0.600	0.585	0.600	0.800	0.600

TABLE III
ACTIVE AND REACTIVE POWER FLOWS

From	$P_{ij}^{\rm true}$	P_{ij}^m	P_{ij}^e	$Q_{ij}^{\rm true}$	Q_{ij}^m	Q_{ij}^e
To	(p.u. MW)			(p.u. MVAr)		
1- 2	0.231	0.231	0.231	-0.131	-0.125	-0.129
1- 4	0.584	0.566	0.561	–	–	–
1- 5	0.509	0.516	0.522	–	–	–
2- 3	0.205	0.191	0.202	-0.064	-0.041	-0.041
2- 4	0.746	0.737	0.749	–	–	–
2- 5	0.352	0.390	0.367	–	–	–
2- 6	0.529	0.515	0.526	–	–	–
3- 5	0.256	0.230	0.269	–	–	–
3- 6	0.547	0.520	0.531	–	–	–

APPENDIX III
DERIVATIVES WITH RESPECT TO PHYSICAL LINE PARAMETERS

In order to simplify the mathematical formulation of the state estimation problem, constraints (4)-(7) are expressed in terms of the network admittance matrix $\boldsymbol{Y} = \boldsymbol{G} + j\boldsymbol{B}$. And consequently, the sensitivities obtained are related to the real and the imaginary parts of the admittance matrix, G_{ij} and B_{ij}, respectively. If the sensitivities with respect to the physical parameters of the lines, resistances (r_{ij}) and reactances (x_{ij}), are required, the chain rule must be used as indicated below.

TABLE IV
LINE DATA

Line #	From To	r_{ij} (p.u.)	x_{ij} (p.u.)	b_{ij}^s (p.u.)
1	1-2	0.10	0.20	0.04
2	1-4	0.05	0.20	0.04
3	1-5	0.08	0.30	0.06
4	2-3	0.05	0.25	0.06
5	2-4	0.05	0.10	0.02
6	2-5	0.10	0.30	0.04
7	2-6	0.07	0.20	0.05
8	3-5	0.12	0.26	0.05
9	3-6	0.02	0.10	0.02
10	4-5	0.2	0.40	0.08
11	5-6	0.10	0.30	0.06

Terms of the admittance matrix are related to the line resistances and reactances as:

$$G_{ij} = \frac{-r_{ij}}{r_{ij}^2 + x_{ij}^2},\ B_{ij} = \frac{x_{ij}}{r_{ij}^2 + x_{ij}^2},\ \forall i\ \forall j \in \Omega_i, \tag{39}$$

and

$$G_{ii} = -\sum_j G_{ij},\ B_{ii} = \sum_j \left(-B_{ij} + b_{ij}^s/2\right),\ \forall i. \tag{40}$$

Let u be the variable for which the partial derivatives are looked for. The sensitivities of the variable u with respect to the resistances (r_{ij}) can be obtained using the chain rule as follows:

$$\begin{aligned}\frac{\partial u}{\partial r_{ij}} &= \frac{\partial G_{ij}}{\partial r_{ij}}\left(\frac{\partial u}{\partial G_{ij}} + \frac{\partial u}{\partial G_{ii}}\frac{\partial G_{ii}}{\partial G_{ij}} + \frac{\partial u}{\partial G_{jj}}\frac{\partial G_{jj}}{\partial G_{ij}}\right)\\ &+ \frac{\partial B_{ij}}{\partial r_{ij}}\left(\frac{\partial u}{\partial B_{ij}} + \frac{\partial u}{\partial B_{ii}}\frac{\partial B_{ii}}{\partial B_{ij}} + \frac{\partial u}{\partial B_{jj}}\frac{\partial B_{jj}}{\partial B_{ij}}\right)\\ &= \frac{\partial G_{ij}}{\partial r_{ij}}\left(\frac{\partial u}{\partial G_{ij}} - \frac{\partial u}{\partial G_{ii}} - \frac{\partial u}{\partial G_{jj}}\right)\\ &+ \frac{\partial B_{ij}}{\partial r_{ij}}\left(\frac{\partial u}{\partial B_{ij}} - \frac{\partial u}{\partial B_{ii}} - \frac{\partial u}{\partial B_{jj}}\right), \forall i\ \forall j \in \Omega_i.\end{aligned} \tag{41}$$

From (39) the derivatives of the admittance matrix terms with respect to resistances (r_{ij}) can be obtained as follows:

$$\frac{\partial G_{ij}}{\partial r_{ij}} = \frac{r_{ij}^2 - x_{ij}^2}{(r_{ij}^2 + x_{ij}^2)^2}, \qquad \frac{\partial B_{ij}}{\partial r_{ij}} = \frac{-2r_{ij}x_{ij}}{(r_{ij}^2 + x_{ij}^2)^2}, \tag{42}$$

whereas from (40), $\frac{\partial G_{ii}}{\partial G_{ij}} = \frac{\partial B_{ii}}{\partial B_{ij}} = -1$.

The terms between parenthesis in equation (41), i.e., the partial derivatives with respect to the elements of the admittance matrix, are the ones obtained in the method proposed in this paper.

Analogously, the sensitivities of the variable u with respect to reactances (x_{ij}) can be obtained as:

$$\begin{aligned}\frac{\partial u}{\partial x_{ij}} &= \frac{\partial G_{ij}}{\partial x_{ij}}\left(\frac{\partial u}{\partial G_{ij}} - \frac{\partial u}{\partial G_{ii}} - \frac{\partial u}{\partial G_{jj}}\right)\\ &+ \frac{\partial B_{ij}}{\partial x_{ij}}\left(\frac{\partial u}{\partial B_{ij}} - \frac{\partial u}{\partial B_{ii}} - \frac{\partial u}{\partial B_{jj}}\right), \forall i\ \forall j \in \Omega_i,\end{aligned} \tag{43}$$

where the derivatives of the admittance matrix terms with respect to reactances (x_{ij}) can be obtained from (39) as follows:

$$\frac{\partial G_{ij}}{\partial x_{ij}} = \frac{2r_{ij}x_{ij}}{(r_{ij}^2 + x_{ij}^2)^2}, \qquad \frac{\partial B_{ij}}{\partial x_{ij}} = \frac{r_{ij}^2 - x_{ij}^2}{(r_{ij}^2 + x_{ij}^2)^2}. \tag{44}$$

If the sensitivities of variable u with respect to the shunt susceptances (b_{ij}^s) are sought for, the following expressions should be used:

$$\begin{aligned} \frac{\partial u}{\partial b_{ij}^s} &= \left.\frac{\partial u}{\partial b_{ij}^s}\right|_0 + \frac{\partial u}{\partial B_{ii}}\frac{\partial B_{ii}}{\partial b_{ij}^s} + \frac{\partial u}{\partial B_{jj}}\frac{\partial B_{jj}}{\partial b_{ij}^s} \\ &= \left.\frac{\partial u}{\partial b_{ij}^s}\right|_0 + \frac{\partial u}{\partial B_{ii}}\frac{1}{2} + \frac{\partial u}{\partial B_{jj}}\frac{1}{2}, \forall i\ \forall j \in \Omega_i, \end{aligned} \tag{45}$$

where $\left.\frac{\partial u}{\partial b_{ij}^s}\right|_0$ are the derivatives obtained using the proposed method. Note also that due to (40), $\frac{\partial B_{ii}}{\partial b_{ij}^s} = \frac{\partial B_{jj}}{\partial b_{ij}^s} = \frac{1}{2}$.

REFERENCES

[1] J. S. Sobieski, J. F. Barthelemy, and K. M. Riley, "Sensitivity of optimal solutions of problems parameters," *AIAA J.*, vol. 20, no. 9, pp. 1291–1299, 1982.

[2] A. V. Fiacco, *Introduction to sensitivity and stability analysis in nonlinear programming*. New York: Academic Press, 1983.

[3] A. Conejo, E. Castillo, R. Mínguez, and R. García-Bertrand, *Decomposition techniques in mathematical programming. Engineering and science applications*. New York: Springer Berlin Heidelberg, 2006.

[4] E. Castillo, A. Conejo, C. Castillo, R. Mínguez, and D. Ortigosa, "A perturbation approach to sensitivity analysis in nonlinear programming," *Journal of Optimization Theory and Applications*, vol. 128, no. 1, pp. 49–74, January 2006.

[5] T. A. Stuart and C. J. Herget, "A sensitivity analysis of weighted least squares state estimation for power systems," *IEEE Transactions on Power Apparatus and Systems*, vol. PA92, no. 5, pp. 1696–1701, Sep-Oct 1973.

[6] I. Hiskens, "Nonlinear dynamic model evaluation from disturbance measurements," *IEEE Transactions on Power Systems*, vol. 16, no. 4, pp. 702–710, 2001.

[7] W. Edwin Liu and S. Lim, "Parameter error identification and estimation in power system state estimation," *IEEE Transactions on Power Systems*, vol. 10, no. 1, pp. 200–209, February 1995.

[8] A. Conejo, E. Castillo, R. Mínguez, and F. Milano, "Locational marginal price sensitivities," *IEEE Transactions on Power Systems*, vol. 20, no. 4, pp. 2026–2033, November 2005.

[9] R. Mínguez and A. J. Conejo, "State estimation sensitivity analysis," in *Proc. 13th IEEE Mediterranean Electrotechnical Conference (MELECON 2006)*, Benalmádena, Málaga (Spain), May. 2006, pp. 956–959.

[10] F. C. Schweppe and J. Wildes, "Power system static state estimation. Part I: Exact model," *IEEE Transactions on Power Apparatus and Systems*, vol. 89, no. 1, pp. 120–125, January 1970.

[11] A. Monticelli, "Electric power system state estimation," *Proceedings of the IEEE*, vol. 88, no. 2, pp. 262–282, 2000.

[12] Reliability Test System Task Force, "The IEEE reliability test system 1996," *IEEE Transactions on Power Systems*, vol. 14, no. 3, pp. 1010–1020, 1999.

[13] A. Abur and A. G. Expósito, *Electric Power System State Estimation. Theory and Implementations*. New York: Marcel Dekker, 2004.

[14] M. S. Bazaraa, H. D. Sherali, and C. M. Shetty, *Nonlinear Programming. Theory and Algorithms*, 2nd ed. New York: John Wiley & Sons, 1993.

[15] D. G. Luenberger, *Linear and Nonlinear Programming*, 2nd ed. Massachusetts: Addison-Wesley, Reading, 1984.

[16] G. B. Sheblé, *Computational auction mechanisms for restructured power industry operation*. Boston: Kluwer Academic Publishers, 1999.

Roberto Mínguez received from the University of Cantabria, Santander, Spain, the Civil Engineering degree, and the Ph.D. degree in Applied Mathematics and Computer Science in September 2000 and June 2003, respectively. During 2004 he worked as Visiting Scholar at Cornell University, New York, under the Fulbright program. He is currently an Assistant Professor of Numerical Methods in Engineering at the University of Castilla-La Mancha.

His research interests are reliability engineering, sensitivity analysis, numerical methods, and optimization.

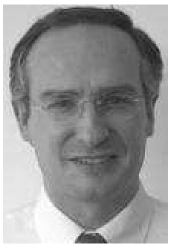

Antonio J. Conejo (F'04) received the M.S. degree from MIT, Cambridge, MA, in 1987, and a Ph.D. degree from the Royal Institute of Technology, Stockholm, Sweden in 1990. He is currently a full Professor at the University of Castilla-La Mancha, Ciudad Real, Spain.

His research interests include control, operations, planning and economics of electric energy systems, as well as statistics and optimization theory and its applications.